

# **B-SPLINE BASED METAMODEL OF THE THERMAL ANALYSIS OF THE WIRE ARC ADDITIVE MANUFACTURING PROCESS**

**Zani, Mathilde (1);  
Montemurro, Marco (1);  
Panettieri, Enrico (1);  
Marin, Philippe (2)**

1: Arts et Métiers Institute of Technology, Université de Bordeaux, CNRS, INRA, Bordeaux INP, HESAM Université, I2M UMR, F-33405 Talence, France;

2: Grenoble Alpes - Laboratoire G-SCOP UMR 5272, F-38000 Grenoble, France

## **ABSTRACT**

Among additive manufacturing processes, wire arc additive manufacturing (WAAM) is one of the most promising methods for manufacturing complex near-net-shape parts, as it allows the layer-by-layer deposition of welded material at a high deposition rate. However, this technology is highly dependent on deposition conditions and thermomechanical phenomena during the process. Therefore, process simulation could be used to analyse the effects of different deposition parameters on the thermomechanical results to optimise the process. However, as the computing time required for this study may become prohibitive, a dedicated strategy is needed to reduce it while maintaining a good level of accuracy. In this study, only the thermal analysis of the process is investigated. An efficient metamodel based on B-spline entities is developed to emulate the thermal response of the WAAM process when building a mild steel four-layer wall structure. Thanks to B-spline entities, the temperature profile at different locations is approximated as a function of a subset of deposition parameters of WAAM process, and the results are compared with the simulated temperature profile resulting from a validation dataset.

**Keywords:** Additive Manufacturing, Industry 4.0, Simulation, Metamodel, B-spline

## **Contact:**

Zani, Mathilde  
I2M laboratory  
France  
mathilde.zani@ensam.eu

**Cite this article:** Zani, M., Montemurro, M., Panettieri, E., Marin, P. (2023) 'B-Spline Based Metamodel of the Thermal Analysis of the Wire Arc Additive Manufacturing Process', in *Proceedings of the International Conference on Engineering Design (ICED23)*, Bordeaux, France, 24-28 July 2023. DOI:10.1017/pds.2023.81

## 1 INTRODUCTION

Additive Manufacturing (AM) processes became one of the main innovations in the Industry 4.0 era. Indeed, such technologies provide environmentally sympathetic manufacturing benefits such as the possibility of manufacturing parts with complex geometries and a significant reduction of material waste (Montevecchi et al., 2016). Among metal AM processes, wire arc additive manufacturing (WAAM) is one of the most promising technologies in terms of deposition rate (Ding et al., 2015) and allows producing large near-shape metal parts with complex geometry by depositing weld beads with a layer-by-layer strategy (Chergui, 2021). Despite these advantages, the quality of parts manufactured by WAAM is highly affected by the thermal and mechanical phenomena occurring during the process, which are influenced by its main parameters. Furthermore, the understanding of the relationships between the physical phenomena and the parameters governing the process (together with the interaction between these parameters) represents a challenging task (Wu et al., 2018; Ding et al., 2015).

Accordingly, process simulation is a powerful tool to undertake such issues, allowing the simulation of the effect of different deposition parameters and, thus, optimizing the process.

From a simulation perspective, WAAM technology is usually simulated with a transient thermomechanical Finite Element (FE) analysis with progressive material addition. However, the computational time associated with this analysis can become prohibitive, especially when the influence of the process parameters on the thermomechanical properties of the material must be integrated in the design process. As discussed by Ding et al. (2011) this is often the cause of a reduction in the effectiveness gains of the WAAM process numerical modelling. Furthermore, due to prohibitive computational costs related to the non-linear thermomechanical FE analysis, such modelling strategy is not suitable for assessing the sensitivity of the temperature field and on the residual strain/stress fields within manufactured parts to the main process parameters. Therefore, suitable abaci to be used during preliminary design phase to predict the behaviour of the resulting material, in terms of stiffness, thermal conductivity, thermal expansion coefficients, etc. as function of the process parameters cannot be obtained in reasonable time when using this kind of modelling strategy. Accordingly, new methods are needed to reduce computational time, while keeping a good level of accuracy. Among the works available in the literature, Ding et al. (2011) proposed a steady state approach tailored for the simulation of large parts with constant deposition speed. In the same perspective, Montevecchi et al. (2017) developed a FE model for thermo-mechanical analyses based on the mesh coarsening technique to reduce the computational costs of the analyses. Michaleris (2014) proposed a hybrid algorithm of element deposition to reduce computational costs. Therefore, a trade-off must be found between the computational costs and the precision required for a given application (Wang et al., 2020).

In this context, metamodels can be efficiently employed to achieve a good balance between accuracy and computational costs. Indeed, metamodels can be specially conceived for capturing the influence of the main parameters of the process on the manufactured parts, and obtaining results having a level of accuracy as good as the one related to non-linear thermomechanical FE models. Generally, a metamodel consists in the definition of a parametric hyper-surface that is capable of approximating (or interpolating) some data (Audoux et al., 2020b; Baillargeon, 2005) without knowing the explicit physical equations of the problem at hand. Among the different existing metamodeling techniques, Non-Uniform Rational Basis spline (NURBS) entities offer many unique advantages (Audoux et al., 2020b) when compared to other metamodeling approaches (Baillargeon, 2005).

In this paper, an efficient metamodel based on B-spline entities and applied to WAAM process thermal simulations is developed to analyse the thermal response of the process when building a mild steel four-layer wall structure. The temperature profile (evaluated during the fabrication of the part) at different locations, i.e., on the regions where thermocouples are located, is approximated as a function of a subset of the main parameters governing the behaviour of the WAAM process. Finally, the simulated temperature profile of a test set of deposition parameters, evaluated by means of FE simulations and compared with the approximated results obtained with the proposed metamodeling strategy.

## 2 THEORETICAL BACKGROUND

To better understand the purposes of this work, this section briefly provides the theoretical backgrounds of NURBS entities, and the main features of the WAAM process, with a special focus on the process parameters involved in the technology and their influence on the thermal history.

## 2.1 NURBS hyper-surfaces

Commonly, NURBS and basis spline (B-spline) entities are used in CAD software to represent highly non-convex curves and surfaces, but with Turner (2005), their use has been generalised to metamodelling. A NURBS hyper-surface is a polynomial-based function defined over a space of dimension  $N$  domain to a space of any dimension  $M$  codomain,  $\mathbf{H} : \mathbb{R}^N \rightarrow \mathbb{R}^M$  (Audoux et al., 2020b). The mathematical formula of a generic NURBS hyper-surface reads:

$$\mathbf{H}(\zeta_1, \dots, \zeta_N) := \frac{\sum_{i_1=0}^{n_1} \dots \sum_{i_N=0}^{n_N} N_{i_1, p_1}(\zeta_1) \times \dots \times N_{i_N, p_N}(\zeta_N) \omega_{i_1, \dots, i_N} \mathbf{P}_{i_1, \dots, i_N}}{\sum_{j_1=0}^{n_1} \dots \sum_{j_N=0}^{n_N} N_{j_1, p_1}(\zeta_1) \times \dots \times N_{j_N, p_N}(\zeta_N) \omega_{j_1, \dots, j_N}}, \quad (1)$$

where  $\zeta_k \in [0, 1]$  is the  $k$ th dimensionless coordinate (or parametric coordinate), whilst  $\omega_{j_1, \dots, j_N}$  are the weights related to the controls points (CPs)  $\mathbf{P}_{i_1, \dots, i_N} = \{P_{i_1, \dots, i_N}^{(1)}, \dots, P_{i_1, \dots, i_N}^{(M)}\}$ . The number of CPs in the  $k = 1, \dots, N$  directions is  $(n_k + 1)$ . In this way, the control points constituting the *control hyper-net* have the coordinates  $P_{i_1, \dots, i_N}^{(j)} \in \mathbb{R}^{(n_1+1) \times \dots \times (n_N+1)}$ ,  $j = 1, \dots, M$ .

For each parametric direction,  $N_{i_k, p_k}(\zeta_k)$  represents the Bernstein's polynomial of order  $p_k$  and defined recursively as (Piegl and Tiller, 1996):

$$N_{i_k, 0}(\zeta_k) = \begin{cases} 1, & \text{if } U_{i_k}^{(k)} \leq \zeta_k \leq U_{i_k+1}^{(k)}, \\ 0 & \text{otherwise,} \end{cases} \quad (2)$$

$$N_{i_k, q_k}(\zeta_k) = \frac{\zeta_k - U_{i_k}^{(k)}}{U_{i_k+q_k}^{(k)} - U_{i_k}^{(k)}} N_{i_k, q_k-1}(\zeta_k) + \frac{U_{i_k+q_k+1}^{(k)} - \zeta_k}{U_{i_k+q_k+1}^{(k)} - U_{i_k}^{(k)}} N_{i_k-1, q_k-1}(\zeta_k), \quad (3)$$

$$i_k = 0, \dots, n_k, \quad q_k = 1, \dots, p_k, \quad k = 1, \dots, N,$$

where each constitutive blending function is defined on the knot vector:

$$\mathbf{U}_{(k)}^T = \{\underbrace{0, \dots, 0}_{p_k+1}, U_{p_k+1}^{(k)}, \dots, U_{m_k-p_k}^{(k)}, \underbrace{1, \dots, 1}_{p_k+1}\}, \quad \mathbf{U}_{(k)} \in \mathbb{R}^{m_k+1}, \quad k = 1, \dots, N, \quad (4)$$

with  $m_k = p_k + n_k + 1$ .

The blending functions are characterised by different interesting properties that can be found in (Piegl and Tiller, 1996). Here, only the *local support property* is highlighted because of its importance for the NURBS-based metamodel of the WAAM process. Thanks to this property, each control point affects only a restricted portion of the domain wherein the NURBS is defined. In this paper, the weights associated to control points are all set to one, and B-spline hyper-surfaces are considered.

## 2.2 Wire arc additive manufacturing

Nowadays, different technologies are employed to better control the WAAM process. The most used one is the cold metal transfer (CMT) that is an improved version of the classical Gas Metal and Tungsten Arc Welding (GMAW/GTMAW) (Rodrigues et al., 2019). In CMT, the droplet deposition is automatically controlled assuring lower heat input of the base material and more stable molten material deposition (Chergui, 2021). However, the final properties of the part are mostly influenced by the deposition parameters and strategy, inter-layer temperature, the high heat inputs, and consequent cooling rates that typically result in residual stresses and deformations. The understanding of the relationships between the physical phenomena and the parameters (together with the interaction between these parameters) represents a challenging task. Moreover, their regulation is fundamental to assure optimum deposition conditions. The parameters that most influence the WAAM process are: (i) **deposition parameters** necessary for the generation of trajectories, corresponding to the layer thickness, the inter-bead distance, the torch speed (also called travel speed, TS), and the inter-layer temperature; (ii) **heat source parameters**, i.e., the average values of the voltage  $U$  and the current  $I$ , representing the power of the welding generator; (iii) **deposition rate**, i.e., the amount of material deposited per unit of time, also related to the Wire Feed Speed (WFS), (Querard, 2019).

All these parameters are not independent, and their influence on the final properties of the part is difficult to understand. Indeed, the energy input EI, whose expression is provided in, Equation (5), is one of the

parameters that most affect the thermal history of deposited layers and the final quality of the part.

$$EI = \frac{\eta UI}{TS} \quad [\text{J/mm}]. \quad (5)$$

This parameter represents the amount of energy provided to the parts by the electric arc and the melting energy of the wire, for a given length traveled by the torch.

To this purpose, FE models have been adopted to analyse these relations and simulate the different phenomena occurring in the WAAM process, as explained in Section 3.

### 3 MODELING AND THERMAL SIMULATION FOR WAAM

The thermal phenomena, occurring during the WAAM process, can be modeled as a transient nonlinear heat transfer problem wherein the heat transfer from the arc to the molten pool is simulated using an equivalent heat source model, which prescribes a heat generation per unit volume in the molten pool region (Montevacchi et al., 2016). For AM simulations, the three dimensional heat source proposed by Goldak et al. (1984) is generally used as it is capable of modeling the three-dimensional phenomena occurring in the molten pool during deposition. In this model, the heat input is represented as a double ellipsoid distribution, as follows:

$$q(x,y,z) = Q \frac{6\sqrt{3}f_\zeta}{a_\zeta b c \pi^{3/2}} e^{-3\left(\frac{x^2}{a_\zeta^2}\right)} e^{-3\left(\frac{y^2}{b^2}\right)} e^{-3\left(\frac{z^2}{c^2}\right)}, \quad (6)$$

with  $\zeta = f$  (front) for  $x \geq 0$  and  $\zeta = r$  (rear) for  $x < 0$ , and  $f_f + f_r = 2$  to ensure continuity in the source origin  $x = 0$ .  $Q(\mathbf{X}, t) = \eta UI$  is the heat input including the various losses due to dissipation, whilst,  $\eta$  indicates the efficiency of the WAAM process, (Ding et al., 2011). A schematic representation of Equation (6) is provided in Figure 1 Another critical issue in the simulation of the WAAM process is

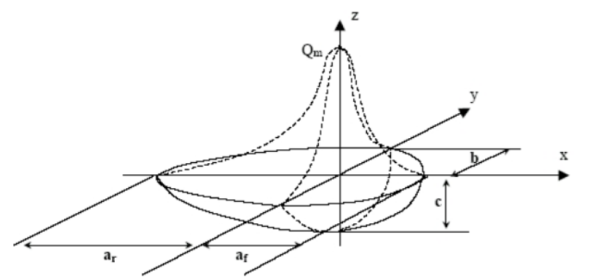


Figure 1. Goldak heat source (Goldak et al., 1984)

the material deposition modeling. Indeed, to simulate the material deposition during the FE simulation of the AM process, an activation algorithm could be employed. In the FE simulations presented in this paper, the progressive elements activation is used. This method, available in ABAQUS® (Smith, 2020), allows replicating the AM process with high fidelity by relating the deposition of elements to the movement of the heat source as function of time and space. More precisely, this method utilizes a geometrical tool-path intersection module that automatically computes the information required for the element activation and the consequent thermal and structural boundary conditions for each given time step (Song et al., 2020), activating the elements when they are intersected by the tool-path. A tool-path is defined as a geometric shape attached to a reference point of the part geometry that moves along a defined path connecting a collection of points in space and time that define the material deposition. For a WAAM technology, the chosen intersection tool unit is of rectangular shape (box), where the material deposition and heat source, are simultaneously applied, (Smith, 2020). The tool-path strategies are shown in Figure 2.

#### 3.1 Finite element model

The FE model of the validation case has been built in ABAQUS® environment by following the guidelines available in the work by Ding et al. (2011). It consists of a four-layer wall, as shown in Figure 3,

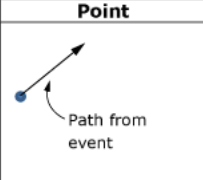
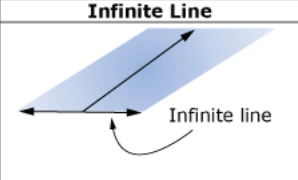
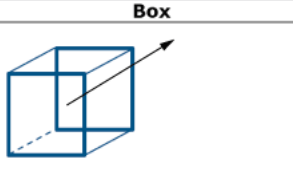
Shape	Point	Infinite Line	Box
<b>Schematic</b>			
<b>Machine tool examples</b>	Point lasers for coarse meshes	Recoater in powder-bed fabrication	Material deposition nozzle in polymer extrusion, wire-feed, laser blob for fine meshes, etc.

Figure 2. Point, infinite line, and box tool-paths (Smith, 2020)

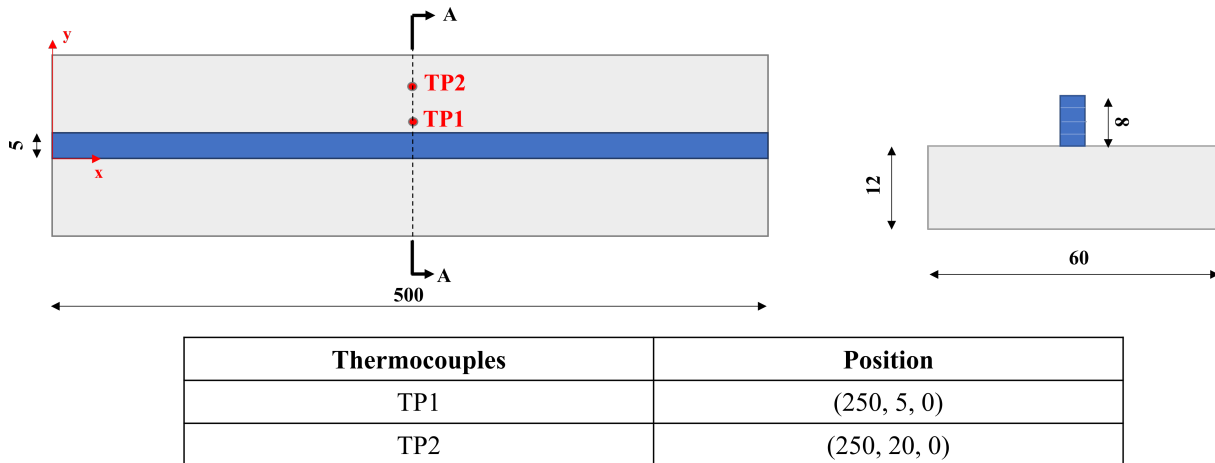


Figure 3. Geometry of the WAAM validation model (dimensions are in mm).

deposited along the center line of the base plate. The material used for both the substrate and the wall is a mild steel with material properties dependent of the temperature taken from literature (Michaleris et al., 1997). During material deposition, the filler material changes its phase from solid to liquid during deposition, and from liquid to solid during cooling. All the other data concerning the material phase changing, deposition and heat source parameters, and heat loss through convection and radiation can be found in Ding et al. (2011).

Lastly, linear brick elements with eight nodes (DC3D8) are used for the thermal simulation with meshes of size 2 mm x 0.833 mm x 0.667 mm for the bead and the area near the welding line, and a coarsened mesh far from the wall to reduce the total number of elements. Moreover, each layer is modelled with three elements in the height. The complete details of the FE model, together with the initial thermal and boundaries conditions and can be found in (Ding et al., 2011). The results of the FE model used for validation purposes are provided in Sec. 5.

### 3.2 WAAM metamodeling database

The goal of the metamodel based on B-spline hyper-surfaces is to emulate the behaviour of the high-fidelity FE model in predicting the temperature value at given locations, i.e., on the nodes where thermocouples TP1 and TP2 are placed as illustrated in Figure 3, as function of some process parameters. Of course, to create the metamodel is necessary to “feed” the algorithm with a database Audoux et al. (2020a). Accordingly, a series of WAAM simulations has to be run by considering suitable intervals for the main process parameters, i.e., the input variables of the metamodel. The values of the selected parameters, are listed in Table 1. The cooling time between two layers is set to 20 s and 50 s, for a total of 200 simulations. The material deposition is effectuated at a constant ratio between the wire feed speed and the travel speed  $R_{WFS/TS} = 8.33$ . The efficiency  $\eta$  of the process is set equal to 0.9 and considered constant for all the combinations of input variables.

As the process parameters vary, there is a modification in the bead behaviour with a consequent change in its temperature history (Chergui, 2021).

Table 1. Values of deposition parameters

TS [mm.s <sup>-1</sup> ]	Q [W]	time [s]
[4.4, 6.2, 8.4, 10, 10.68, 11, 11.2, 12, 13.2, 16.4]	[364, 447.6, 571.1, 700.3, 849.4, 890.1, 1282.3, 1537.4, 1826.3, 2302.2]	[0, 992]

The FE model for the creation of the dataset is a four-layer wall deposited on a substrate of a 200 mm length. The model is a reduced version of the FE model used for validation and presented in section 3.1. The model implementation is the same as that used for validation. Since in this case, the interest is in creating a data-set for the metamodel construction, the heat source and its respective parameters are kept constant and equal to the values taken from (Ding et al., 2011) for simplicity. Moreover, the time step is considered equal to  $t_{inc} = 1$  sec for all the simulation to reduce the computational costs. Finally, the geometry of the model, which should vary as the deposition parameters change (i.e.,  $h$  and  $w$  of the bead change inversely and directly proportional to the EI variation), is kept constant. This simplifying assumption is justified because the deposition of the material occurs at a constant ratio  $R_{WFS/TS}$ , and with the progressive elements deposition modeling. For more details on this assumption the interested reader is addressed to (Cambon, 2021).

The temperature history during deposition is recovered only at the locations of the two thermocouples TP1 and TP2 shown in Figure 3, for each combination of the input parameters listed in Table 1, and the all database is used as training set for the metamodel explained in section 4.

#### 4 METAMODEL BASED ON BASIS SPLINE ENTITIES

The use of B-spline hyper-surfaces as a tool for creating a metamodel allows for generating a hyper-surface capable of fitting a given set of target points (TPs)  $X_i$ . The algorithm, originally implemented in C++ and Matlab languages by Audoux et al. (2020a) has been coded in a Python programming language and generalised to any combination of dimensions  $N$  and  $M$  of the B-spline hyper-surface domain and codomain, respectively. The algorithm is divided into two parts:

- A library containing all the functions needed to evaluate the hyper-surface. The different functions are based on the NURBS book (Piegl and Tiller, 1996) algorithm, and on the already implemented NURBS code at I2M laboratory (Montemurro and Catapano, 2019; Audoux et al., 2020a; Costa et al., 2021);
- A main script containing the main inversion and optimisation procedure for evaluating the control points of the hyper-surface according to the strategy presented by Audoux et al. (2020b), and the point of the hyper-surface.

The flowchart illustrated in Figure 4 summarises the main steps of the algorithm for generating the metamodel based on B-spline hyper-surfaces. Once the input parameters have been supplied by the user in terms of number of control points, size and components of knot vectors along each parametric direction, degree of the basis functions and the dimensionless design parameters (Audoux et al., 2020b), several routines are called to evaluate the basis functions, the optimal values of the control points (constituting the control hyper-net), and, then, the hyper-surface. The database of TPs is determined via numerical analyses conducted via the FE model discussed in Sec. 3.2 before calculating the optimal value of the coordinates of the control points of the B-spline hyper-surface according to the strategy presented by Audoux et al. (2020b). It is noteworthy that all the input variables listed in Table 3.2 have been normalised to get values in the interval  $[0, 1]$ . In this paper, the algorithm proposed by Audoux et al. (2020b), implemented in Python in this work and generalised to the case of a general hyper-surface with  $N$  input variables and  $M$  outputs, is applied to the simulation of the WAAM process on the benchmark problem presented in Sec. 3.2 to approximate the thermal history  $T(t, TS, Q)$  at the two thermocouples for different combinations of input variables  $t$ ,  $Q$  and  $TS$ . The database of TPs is stored in the form of a matrix with dimensions of the type

$$\mathbf{Q}_{s_1, s_2, s_3} = (T(t_{s_1}, TS_{s_2}, Q_{s_3})), \quad s_k = 0, \dots, r_k, \quad (7)$$

where  $r_k$  is the number of TPs along the  $k$ -th parametric direction related to the  $k$ -th input variable. The optimal value of the coordinates of the control points of the B-spline hyper-surface is calculated according to the iterative procedure discussed by Audoux et al. (2020b).



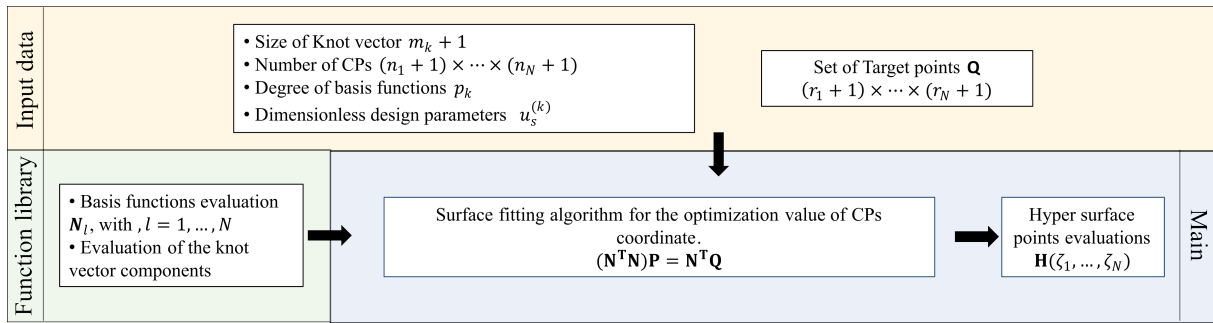


Figure 4. Algorithm flowchart. The hyper-surface surface fitting problem for the optimization of the CPs coordinates is taken from (Audoux et al., 2020b)

The domain for the hyper surface in  $\mathbb{R}^3$  is an unit hyper-cube, whereas the codomain is a topological space simply connected that directly derives from the numerical results. In this research the codomain is the whole set of real numbers.

## 5 RESULTS AND DISCUSSION

The numerical results of the 3D FE model presented in Section 3.1 have been compared to the experimental ones taken from Ding et al. (2011). More precisely, the comparison is carried out in terms of nodal temperature histories for the two thermocouples TP1 and TP2. From Figure 5, it is evident that the temperature history curves obtained numerically are in good agreement with the reference ones. Once

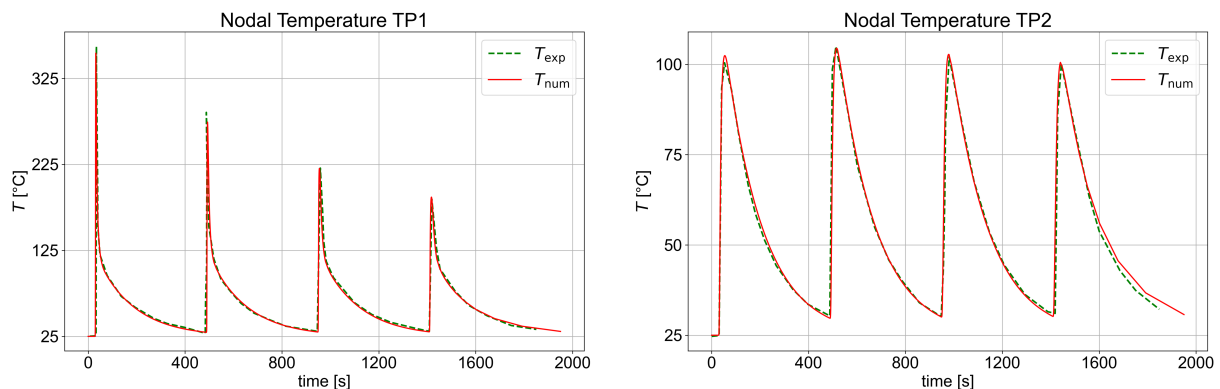


Figure 5. Comparison between the numerical data and the experimental data (Ding et al., 2011) in thermocouples TP1 and TP2.

the numerical model has been validated in terms of temperature evolution, the thermal history  $T(t, TS, Q)$  at the two thermocouples is approximated using the B-spline metamodel. For the sake of brevity, the results are shown only for the thermocouple TP1. Figure 6 shows the contour plots of the temperature of the thermocouple TP1 calculated with the metamodel based on B-spline hyper-surfaces as function of the input variables  $t, Q, TS$ . For both cases, the relative error is lower than 0.5%, resulting, thus, in an accurate prediction of the fitting hyper-surface. Moreover, the computational time to obtain the results from the metamodel is almost 100 % lower than the computational cost of the FE simulations.

Once the metamodel is created, it can be generalized to any set of parameters within the training set variation ranges, and results can be obtained without making use of time-consuming FE simulations. For this reasons, four sets of  $(TS, Q)$  not included in the initial set of TPs used to build the database, have been chosen to evaluate the accuracy of the approximated method. The results of the metamodel obtained for four parameter sets are shown in 7. As mentioned before, the results are only shown for the thermocouple TP1. Overall, the approximated temperature history match quite well the simulated results. However, a difference in the graphical discontinuities can be appreciated, especially close to the peaks and the local minimums of the plots. This difference is due to the behaviour of B-spline entities, which are not able to approximate distributions of data characterised by strong non-linearities and/or

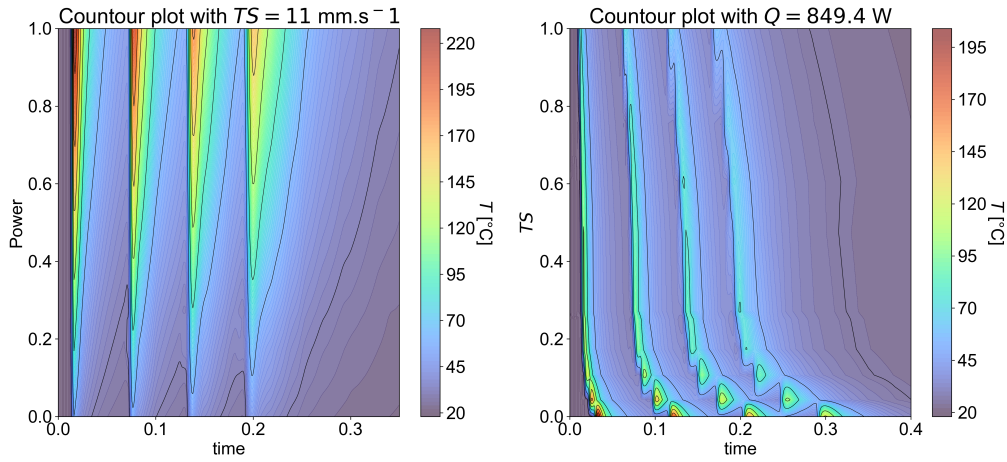


Figure 6. Contour plot of the nodal temperature for thermocouple TP1 resulting from the B-spline hyper-surface for a constant  $TS$  (on the left) and a constant power (on the right).

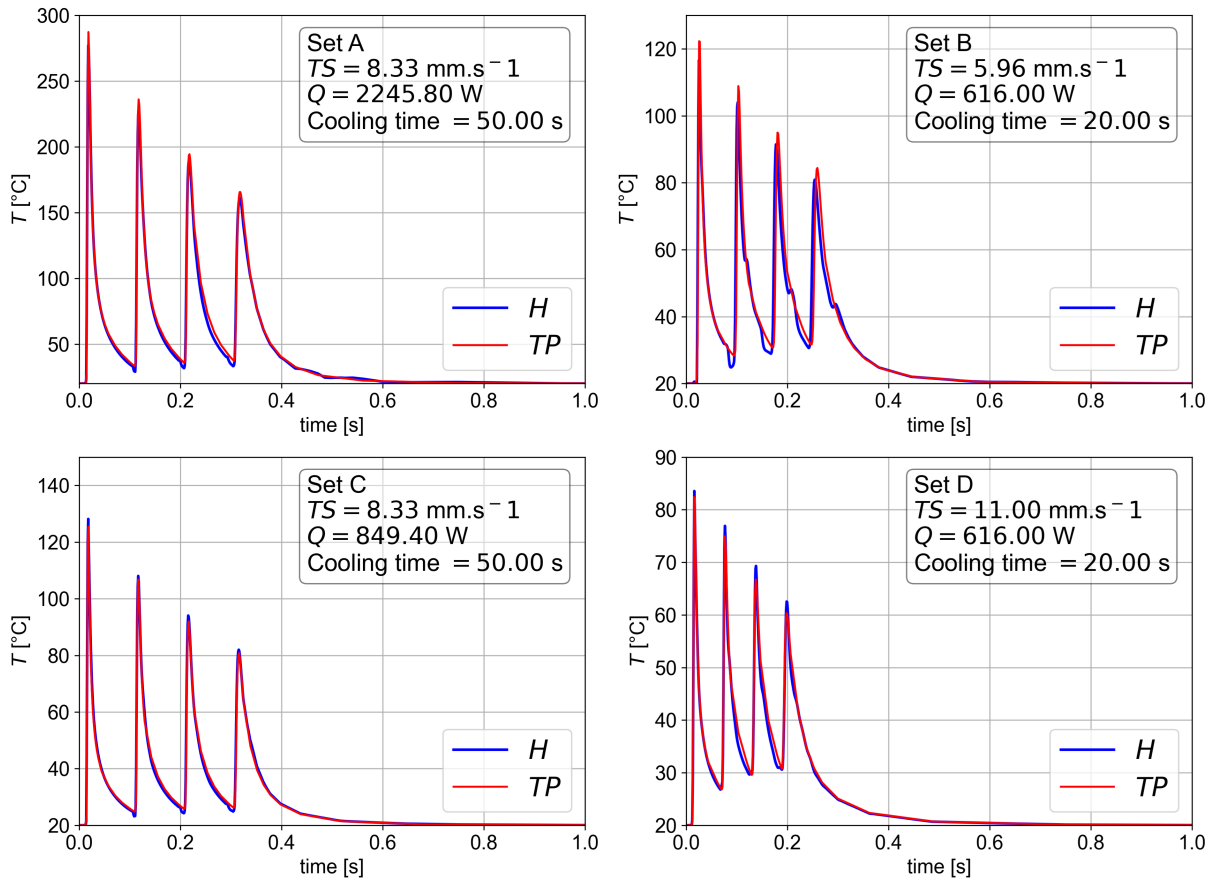


Figure 7. Temperature history at thermocouple TP1 for the four sets of deposition parameters constituting the validation set.

discontinuities on the local tangent vector direction. As discussed by Audoux et al. (2020b), this issue can be overcome by including the inner components of the knot vector among the design variables and, possibly, the weights related to each control points, considering, thus, the most general case of NURBS hyper-surfaces.



## 6 CONCLUSION

In this paper, a metamodel based on B-spline entities has been applied to a physical AM problem to approximate the temperature history at different locations of the 3D model. The applied metamodel is taken from (Audoux et al., 2020b), and coded in python programming language and generalised to any combination of dimensions  $N$  and  $M$  of the B-spline hyper-surface domain and codomain, respectively. As far as the numerical model is concerned, it consists of a rectangular thin four-layer wall also taken from literature (Ding et al., 2011), and tested for different combinations of input variables, i.e., the time  $t$ , the travel speed TS, and the power  $Q$  of the heat source. Overall, the results provided by the FE model and those resulting from the B-spline-based metamodel are in good agreement with a relative error of 0.5 %. Furthermore, a comparison between the approximated temperature profile obtained for sets of parameters not present in the initial database, and the profile obtained from simulation has been performed. It highlighted that the approximated results are able to predict the numerical one even if some discrepancies are present due to the chosen approximation method.

This study shows that metamodeling strategies are promising to approximate and predict the thermal response of the WAAM process for different combinations of the input variables without solving the entire numerical model, and globally give satisfactory results. However, some issues remain to be solved. The B-spline entities are not capable to correctly approximate dataset characterised by strong non-linearity and/or discontinuities in the first partial derivative along each direction. To overcome this issue, the presented metamodeling strategy should be extended to the most general case of NURBS entities by including the weights related to each control point and the inner components of the knot vectors among the design variables. Research is ongoing on this aspect.

## ACKNOWLEDGMENTS

M. Zani is grateful to French National Research Agency for supporting this work through the research project KAM4AM (Fabrication Assistée Par La Connaissance Et L'intelligence Artificielle) ANR-20-CE10-0012-01

## REFERENCES

- Audoux, Y., Montemurro, M. and Pailhès, J. (2020a), "A metamodel based on non-uniform rational basis spline hyper-surfaces for optimisation of composite structures", *Composite Structures*, Vol. 247, p. 112439, <https://doi.org/10.1016/j.compstruct.2020.112439>.
- Audoux, Y., Montemurro, M. and Pailhès, J. (2020b), "Non-uniform rational basis spline hyper-surfaces for metamodeling", *Computer Methods in Applied Mechanics and Engineering*, Vol. 364, p. 112918, <https://doi.org/10.1016/j.cma.2020.112918>.
- Baillargeon, S. (2005), "Le krigeage: revue de la théorie et application à l'interpolation spatiale de données de précipitations, mémoire présenté pour l'obtention du grade de maître ès sciences (m. sc.)", *Université de Laval, Faculté des Sciences et de Génie, Québec*.
- Cambon, C. (2021), *Étude thermomécanique du procédé de fabrication métallique arc-fil : approche numérique et expérimentale*, Theses, Université Montpellier.
- Chergui, M.A. (2021), *Simulation Based deposition Strategies Evaluation and Optimization in Wire Arc Additive Manufacturing*, Theses, Université Grenoble Alpes.
- Costa, G., Montemurro, M. and Pailhès, J. (2021), "Nurbs hyper-surfaces for 3d topology optimization problems", *Mechanics of Advanced Materials and Structures*, Vol. 28 No. 7, pp. 665–684, <https://doi.org/10.1080/15376494.2019.1582826>.
- Ding, D., Pan, Z., Cuiuri, D. and Li, H. (2015), "Wire-feed additive manufacturing of metal components: technologies, developments and future interests", *The International Journal of Advanced Manufacturing Technology*, Vol. 81, pp. 465–481, <https://doi.org/10.1007/s00170-015-7077-3>.
- Ding, J., Colegrove, P., Mehnen, J., Ganguly, S., Sequeira Almeida, P., Wang, F. and Williams, S. (2011), "Thermo-mechanical analysis of wire and arc additive layer manufacturing process on large multi-layer parts", *Computational Materials Science*, Vol. 50 No. 12, pp. 3315–3322, <https://doi.org/10.1016/j.commatsci.2011.06.023>.
- Goldak, J., Chakravarti, A. and Bibby, M. (1984), "A new finite element model for welding heat sources", *Metallurgical transactions B*, Vol. 15 No. 2, pp. 299–305, <https://doi.org/10.1007/BF02667333>.
- Michaleris, P. (2014), "Modeling metal deposition in heat transfer analyses of additive manufacturing processes", *Finite Elements in Analysis and Design*, Vol. 86, pp. 51–60, <https://doi.org/10.1016/j.finel.2014.04.003>.
- Michaleris, P., DeBiccari, A. et al. (1997), "Prediction of welding distortion", *Welding Journal-Including Welding Research Supplement*, Vol. 76 No. 4, p. 172s.

- Montemurro, M. and Catapano, A. (2019), “A general b-spline surfaces theoretical framework for optimisation of variable angle-tow laminates”, *Composite Structures*, Vol. 209, pp. 561–578, <https://doi.org/10.1016/j.compstruct.2018.10.094>.
- Montevecchi, F., Venturini, G., Grossi, N., Scippa, A. and Campatelli, G. (2017), “Finite element mesh coarsening for effective distortion prediction in wire arc additive manufacturing”, *Additive Manufacturing*, Vol. 18, pp. 145–155, <https://doi.org/10.1016/j.addma.2017.10.010>.
- Montevecchi, F., Venturini, G., Scippa, A. and Campatelli, G. (2016), “Finite element modelling of wire-arc-additive-manufacturing process”, *Procedia Cirp*, Vol. 55, pp. 109–114, <https://doi.org/10.1016/j.procir.2016.08.024>.
- Piegl, L. and Tiller, W. (1996), *The NURBS book*, Springer Science & Business Media, <https://doi.org/10.1007/978-3-642-97385-7>.
- Querard, V. (2019), *Réalisation de pièces aéronautiques de grandes dimensions par fabrication additive WAAM*, Theses, École centrale de Nantes.
- Rodrigues, T.A., Duarte, V., Miranda, R.M., Santos, T.G. and Oliveira, J.P. (2019), “Current status and perspectives on wire and arc additive manufacturing (waam)”, *Materials*, Vol. 12 No. 7, <https://doi.org/10.3390/ma12071121>.
- Smith, M. (2020), “Abaqus/standard user’s manual, version 6.20”, .
- Song, X., Feih, S., Zhai, W., Sun, C.N., Li, F., Maiti, R., Wei, J., Yang, Y., Oancea, V., Brandt, L.R. et al. (2020), “Advances in additive manufacturing process simulation: Residual stresses and distortion predictions in complex metallic components”, *Materials & Design*, Vol. 193, p. 108779.
- Turner, C.J. (2005), *HyPerModels: hyperdimensional performance models for engineering design*, The University of Texas at Austin.
- Wang, L., Chen, X., Kang, S., Deng, X. and Jin, R. (2020), “Meta-modeling of high-fidelity fea simulation for efficient product and process design in additive manufacturing”, *Additive Manufacturing*, Vol. 35, p. 101211, <https://doi.org/10.1016/j.addma.2020.101211>.
- Wu, B., Pan, Z., Ding, D., Cuiuri, D., Li, H., Xu, J. and Norrish, J. (2018), “A review of the wire arc additive manufacturing of metals: properties, defects and quality improvement”, *Journal of Manufacturing Processes*, Vol. 35, pp. 127–139, <https://doi.org/10.1016/j.jmapro.2018.08.001>.